Hydrogeology Journal (2019) 27:1581–1596
https://doi.org/10.1007/s10040-019-01955-8

REPORT

Construction of a conceptual model for confined groundwater flow in the Gunii Khooloi Basin, Southern Gobi Region, Mongolia

Batdemberel Bayanzul[1,2] · Kengo Nakamura[2] · Isao Machida[3] · Noriaki Watanabe[2] · Takeshi Komai[2]

Received: 6 August 2018 / Accepted: 19 February 2019 / Published online: 12 March 2019

Abstract

Groundwater plays a vital role in the arid Southern Gobi Region (SGR) of Mongolia. It is the only source of water supply and is largely utilized for mining operations, such as those at Oyu Tolgoi Mine. The area is expected to face severe water shortages for mining and drinking water, which may be related to changes in groundwater recharge due to climate change. Understanding the geochemical evolution of groundwater and recharge mechanisms is thus paramount for water resource management. In this study, for the first time, chemical and isotopic approaches have been used to characterize the groundwater origin and its associated recharge processes in the Gunii Khooloi basin, which is located in the SGR. Shallow groundwater is mainly characterized by Na(HCO_3) and NaCl type; however, Gunii Khooloi aquifer is classified as NaCl type with high electrical conductivity. The stable isotope composition of the water in the deep Cretaceous confined aquifer shows depletion in ^{2}H and ^{18}O relative to modern rainfall and the Quaternary shallow aquifer, which indicates a weak interaction between the two aquifers. Modern groundwater was identified in the shallow streambed aquifer, probably due to the direct infiltration of rainfall. On the other hand, ^{14}C ages in the deep groundwater range from 2,800 to 33,500 years, which suggests that this is paleowater that was recharged during the glacial age. The results indicate that there is a need for strategic groundwater management in the Gunii Khooloi basin.

Keywords Hydrochemistry · Groundwater origin · Stable isotopes · Arid regions · Mongolia

✉ Batdemberel Bayanzul
batdemberel@must.edu.mn

Kengo Nakamura
kengo.nakamura.e8@tohoku.ac.jp

Isao Machida
i-machida@aist.go.jp

Noriaki Watanabe
noriaki.watanabe.e6@tohoku.ac.jp

Takeshi Komai
komai@mail.kankyo.tohoku.ac.jp

[1] School of Geology and Mining Engineering, Mongolian University of Science and Technology, Ulaanbaatar 14191, Mongolia

[2] Graduate School of Environmental Studies, Tohoku University, Aoba, Aramaki, Aoba-Ku, Sendai 980-8579, Japan

[3] Groundwater research group, Geological Survey of Japan, Advanced Industrial Science and Technology (AIST), Central 7, 1-1-1 Higashi, Tsukuba-shi, Ibaraki 305-8567, Japan

Introduction

Continued population growth, the development of mining industries, and recent climate change are putting water resources under pressure in arid and semi-arid regions (e.g., Ragab and Prudhomme 2002; Bahir et al. 2018; Ouhamdouch et al. 2016, 2018). The Gobi Desert is one of the largest deserts in the world, which expands across northern China and the southern part of Mongolia (Fig. 1a). The largest mineral deposits of Mongolia are located in the Southern Gobi Region (SGR).

The groundwater in the SGR is in a critical situation. In this region, shallow groundwater serves as the only source of water supply for drinking, domestic and livestock watering; while deep groundwater (Gunii Khooloi aquifer) is largely utilized by exploration and mining companies such as the Oyu Tolgoi Mine (southern part of the Gunii Khooloi basin, Fig. 1b). The Gunii Khooloi basin has recently been the focus of attention due to increasing water demand by the Oyu Tolgoi Mine and its resulting environmental impact. Local communities are

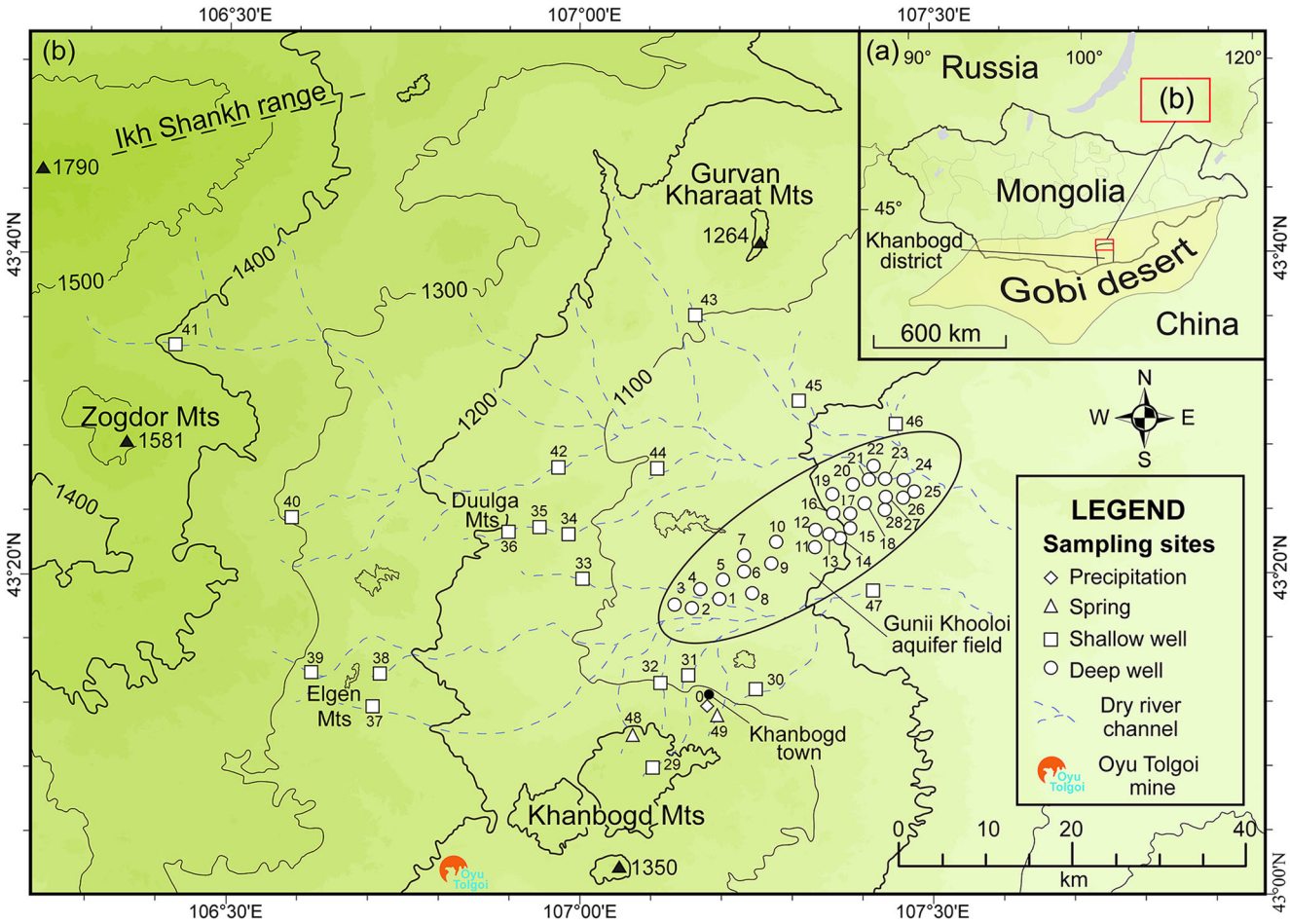

Fig. 1 Map showing: **a** location of the study area and its relationship to the Khanbogd district and Gobi Desert, **b** topography of the Gunii Khooloi basin and sampling locations. The contour lines represent elevation (m asl)

concerned that the groundwater that they always use may dry up or be contaminated, thereby restricting their domestic usage and negatively impacting their livelihoods as herders.

Over the past few decades, the Mongolian government and the Oyu Tolgoi company have conducted hydrogeological exploration for assessment and development of the water resources in the Gunii Khooloi basin, and for understanding the hydrogeological conditions of the study area (Munkhbaatar et al. 2004; Tuvdendorj et al. 2008). Analysis of the aquifer system and hydrogeological conditions together with geochemical and isotopic techniques can provide information on the groundwater sources and their associated recharge processes (Coplen et al. 2000; Mahlknecht et al. 2004; Glynn and Plummer 2005; Ma et al. 2009).

Therefore, although significant isotopic and hydrogeochemical surveys have been conducted over the past decade in the middle and southern part of the Gobi Desert (northern China) such as the Shiyang River basin (Ma et al. 2005), the Badain Jaran Desert (Gates et al. 2008), the Heihe River basin (Yang et al. 2011), the Dunhuang basin (Ma et al. 2013) and the Hexi Corridor (Wang et al. 2017) the northern part of the Gobi Desert (Southern Gobi Region, Mongolia) is still not well understood. Comprehensive investigations to understand groundwater geochemical evolution, recharge mechanisms, and the origin of groundwater and groundwater age that combine chemistry and isotopic indicators are also few or nonexistent in Mongolia.

Through a hydrogeological survey of shallow and deep aquifers in the Gunii Khooloi basin using geochemical and isotope methods, the current study sought to clarify (1) shallow and deep groundwater characteristics, (2) groundwater age, and (3) the groundwater origin through assessment of a combination of isotopic data and hydrogeological information.

Study area

General setting

The Gunii Khooloi basin is located in the Khanbogd district, SGR (northern part of the Gobi Desert), between 106°10′E to 108°05′E and 43°05′N to 43°55′N with an

area of approximately 7,100 km^2 (Fig. 1a). The area is surrounded by the Khanbogd Mountains (peak elevation 1,350 meters above mean sea level (m asl) to the south, the Zogdor Mountains (peak elevation 1,581 m asl) to the west, and the Ikh Shankh range (peak elevation 1,790 m asl) and Gurvan Kharaat Mountains (peak elevation 1,264 m asl) to the northwest and northeast (Fig. 1b). Surface runoff is ephemeral in the basin, with some permanent springs and temporary surface streams originating from the surrounding high mountains during summer and autumn rain events. Runoff from all of these flows traverse the surface above the Gunii Khooloi aquifer footprint.

Yang and Scuderi (2010) concluded that a cold and wetter climate prevailed between about 41 and 30 ka before present (BP), and generally drier conditions prevailed from 24 to 18 ka BP, in the Gobi Desert. From the beginning of the Holocene, wetter conditions prevailed until about 3.5 ka BP, interrupted by three shorter dry and cold reversals (Felauer et al. 2012). Most studies from northern China and southern Mongolia have concluded that in the late Holocene (from 3.5 ka BP to present), the climate changed to dry and warm conditions (Chen et al. 2016; Stauch 2016; Lehmkuhl et al. 2018).

At present, the region is climatically characterized by an extremely arid desert climate (Kottek et al. 2006) that is hot in the summer and cold in the winter. According to observational data from 1977 to 2016 at the Khanbogd meteorological station, the mean annual temperature is approximately 7.5 °C with an average monthly temperatures of –11.6 °C (January) and 24.9 °C (July). Precipitation is influenced by Asian monsoon, with 80% of precipitation from June to September. The mean annual rainfall measured at the Khanbogd station was only 98.8 mm (during the last 40 years), and potential evaporation is approximately 2,900 mm/year.

Geology and hydrogeology

The study area is situated in the Gurvansaikhan island arc terrane, which is one of the 44 terranes of Mongolia, in the center of the Central Asian Orogenic Belt (CAOB; Badarch et al. 2002). The CAOB is one of the largest orogens in the world (Fig. 2a), and it is surrounded by the Siberian and East European (Baltica) cratons to the north and the Tarim–North China (Sino–Korean) cratonic blocks to the south (Şengör et al. 1993; Jahn et al. 2000; Windley et al. 2007). The Gurvansaikhan terrane is formed through a complex process of island arc accretion and rifting of paleo–ocean. From the Neoproterozoic to the Silurian, the area was a Paleo–Asian Ocean margin setting (Fig. 2b), which was later subjected to subduction, rifting and finally accretion to form a continental environment until the Cretaceous period (Fig. 2c).

In terms of the geotectonic characteristics of the Gurvansaikhan terrane, geological units can be described: volcanic complex, alkaline granites and Cretaceous sedimentary basin. The uplift of the Ikh Shankh Mountain range, Duulga Mountain, Gurvan Kharaat and Ulaan Tolgoi ridges (volcanic complex) and Khanbogd Mountains (alkaline granite) occurred from the Devonian to Permian period and created the embryonic form of the Cretaceous sedimentary basin (Fig. 2d). As a result of this system activity, intensive denudation and erosion from the mountains led to a significant transfer of clastic material to the depressions of the Gunii Khooloi basin. This deposition, mainly from the Cretaceous to the Quaternary period, of thick alluvial, diluvia–proluvial sediments, and some aeolian and lacustrine deposits, led to the formation of the aquifer systems.

The Gunii Khooloi basin contains two main aquifer systems, a shallow streambed aquifer and a main deep confined aquifer (Gunii Khooloi aquifer, Fig. 3a). The shallow streambed aquifer system in this region is formed from highly permeable Quaternary alluvium, diluvial–proluvial sand, cobbles and gravel sediments with a total thickness from less than 8 to 20 m in some places. This aquifer system constitutes a single layer of unconfined aquifer and the water table ranges from 0.5 to 7 m below the ground surface (m bgs). The specific capacity is approximately 0.5–3.5 L/s m (Munkhbaatar et al. 2004). Most of the herders' hand-dug wells are located within these dry river channels, which are mainly used for husbandry and domestic purposes.

The Gunii Khooloi aquifer, in the Bayanshiree series, consists of Upper Cretaceous sedimentary formations and is distributed in the north of the Khanbogd Mountains, spreading out within the Gunii Khooloi basin. It is composed of a stratified sequence of sand, gravel, weakly consolidated sandstone, siltstone, gravelstone and conglomerate, which are interbedded with thin clay layers. The confining layers, Tsogt-Ovoo and Ulaan Gobi, are impermeable or weakly permeable layers formed by clayey sandstone and conglomerate with some lenses of clay, which indicates there are no vertical flows existing between the shallow and deep aquifers. The series has less thickness at the edges of the valley than at the central part of the deep aquifer, where it reaches a thickness of 160–260 m. Therefore, these formations make this Gunii Khooloi aquifer a confined aquifer. The Gunii Khooloi aquifer thickness and permeability increase continuously from the southwest to the northeast. Sandstone and conglomerate associated lithology of the Sainshand series are underlain by the deep aquifer and are gradually dipping in the same direction. The Gunii Khooloi aquifer is located at 115–287 m bgs, and the thickness is generally from 55 to 243 m. The total hydraulic head varies from 66 to 175 m, and the transmissivity ranges from 112 to 2,800 m^2/day (Tuvdendorj et al. 2008). There are also two groundwater flow directions observed (Tuvdendorj et al. 2008), which are southwest to northeast and northwest to southeast (Fig. 3b).

Near the central part of the Gunii Khooloi aquifer (left side of point 7 in Fig. 4), where the basement rocks have been

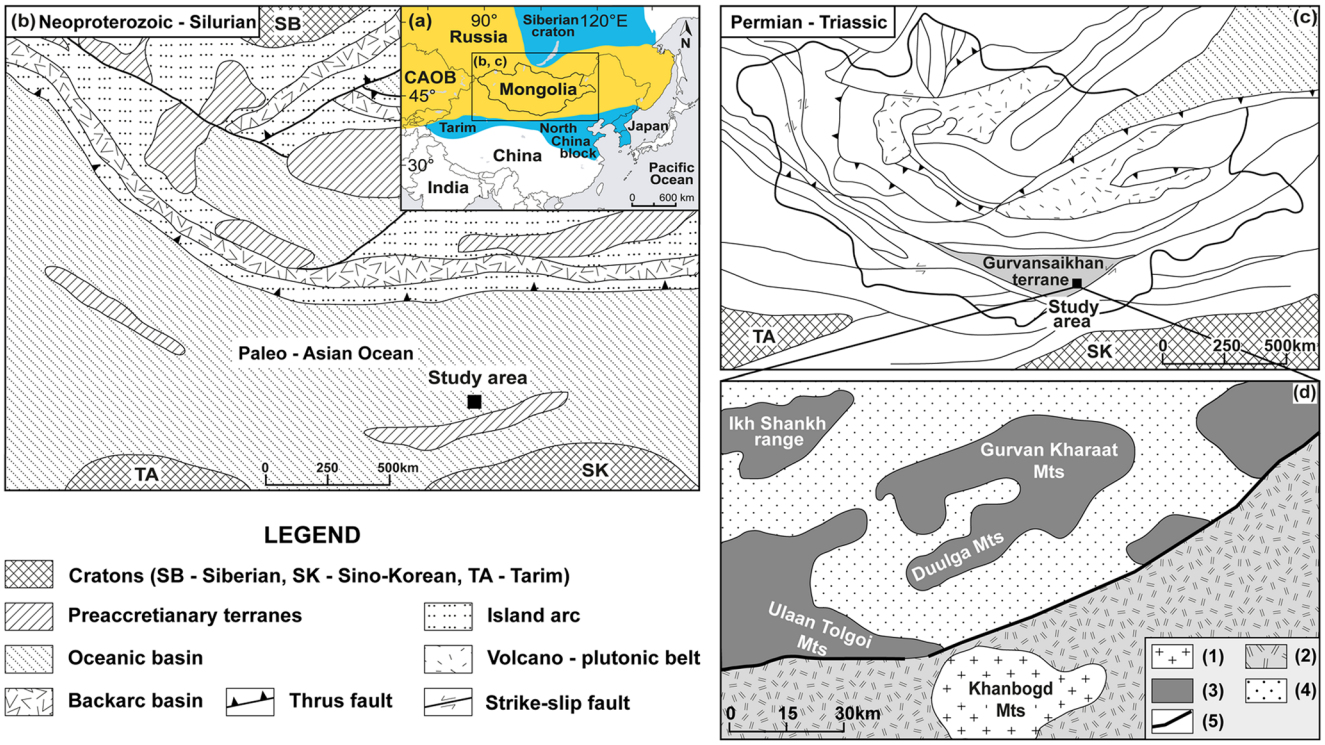

Fig. 2 **a** Simplified tectonic map showing the location of the study area and the main tectonic components. The yellow area indicates the Central Asian Orogenic Belt (CAOB). Blue areas indicate neighboring Archean to Mesoproterozoic cratons (modified after Jahn et al. 2000). **b–c** Simplified evolutionary model of terrane accretion and amalgamation in Mongolia and neighboring regions (modified after Badarch et al. 2002). **d** Geological sketch map of the study area. Legend: (1) Khanbogd alkali granite pluton, (2) segments of rift zones overlapped with younger sediments, (3) Hercynides and complexes of active continental margin therein, (4) Mesozoic and Cenozoic Basins, and (5) faults (modified after Kovalenko et al. 2006)

uplifted due to the geological setting of the basin, many thin clayey layers are found in the aquifer, which makes it more clayey overall. This narrow uplift may also cause discontinuity in the center of the basin, dividing the deep aquifer into two different parts with various hydrogeological parameters. The average thickness of the deep aquifer in the southwestern part is consequently 88 m, and 153 m in the northeastern part. In the southwestern part, the hydraulic head is 980 m asl and transmissivity is 327 m^2/day. In contrast, in the northeastern part of the deep aquifer, the hydraulic head and transmissivity are 930 m asl and 957 m^2/day, respectively (Tuvdendorj et al. 2008). This allows thickness and transmissivity of the aquifer at the western part to be lower than those in the eastern part; however, the recharge area of the deep aquifer is still unknown.

Materials and methods

Wells, springs and precipitation in the Gunii Khooloi basin were sampled twice (in September, 2016 and in June, 2017) for chemical and isotope analysis. Major chemical composition and stable isotope samples were collected from late September to the beginning of October 2016. These included one precipitation sample (labeled 'Rain' in Table 1) and 49 groundwater samples (2 springs, 19 shallow hand-dug wells and 28 deep production wells). The rainfall sample was collected from Khanbogd *soum* center (sample No. 0 in Fig. 1).

Two spring water samples (labeled 'Spring' in Table 1, samples 48 and 49 in Fig. 1) were collected from the Khanbogd Mountain. Nineteen shallow-aquifer groundwater samples were collected from hand-dug wells at depths of less than 10 m (wells used for domestic purposes, labeled 'Shallow' in Table 1). Most of the shallow groundwater wells are located in the recharge area of the Gunii Khooloi aquifer. The Gunii Khooloi aquifer water samples were obtained from 28 deep production wells (>245 m bgs, serving as water supply for the Oyu Tolgoi mine, labeled 'Deep' in Table 1). To insure consistent in situ conditions of representative samples, all production wells had been pumping continuously for several hours or days prior to sampling. All water taken from the shallow hand-dug wells was not stagnant inside the wells for long because the wells are used for livestock every day.

Water pH (DKK–TOA HM–30, three-point calibration), electrical conductivity (EC; DKK–TOA CM–31P; calibrated with 0.1 N sodium chloride standard solution) and dissolved oxygen (DO; DKK-TOA DO-31P; calibrated with sodium sulfite solution) were determined in the field. Alkalinity

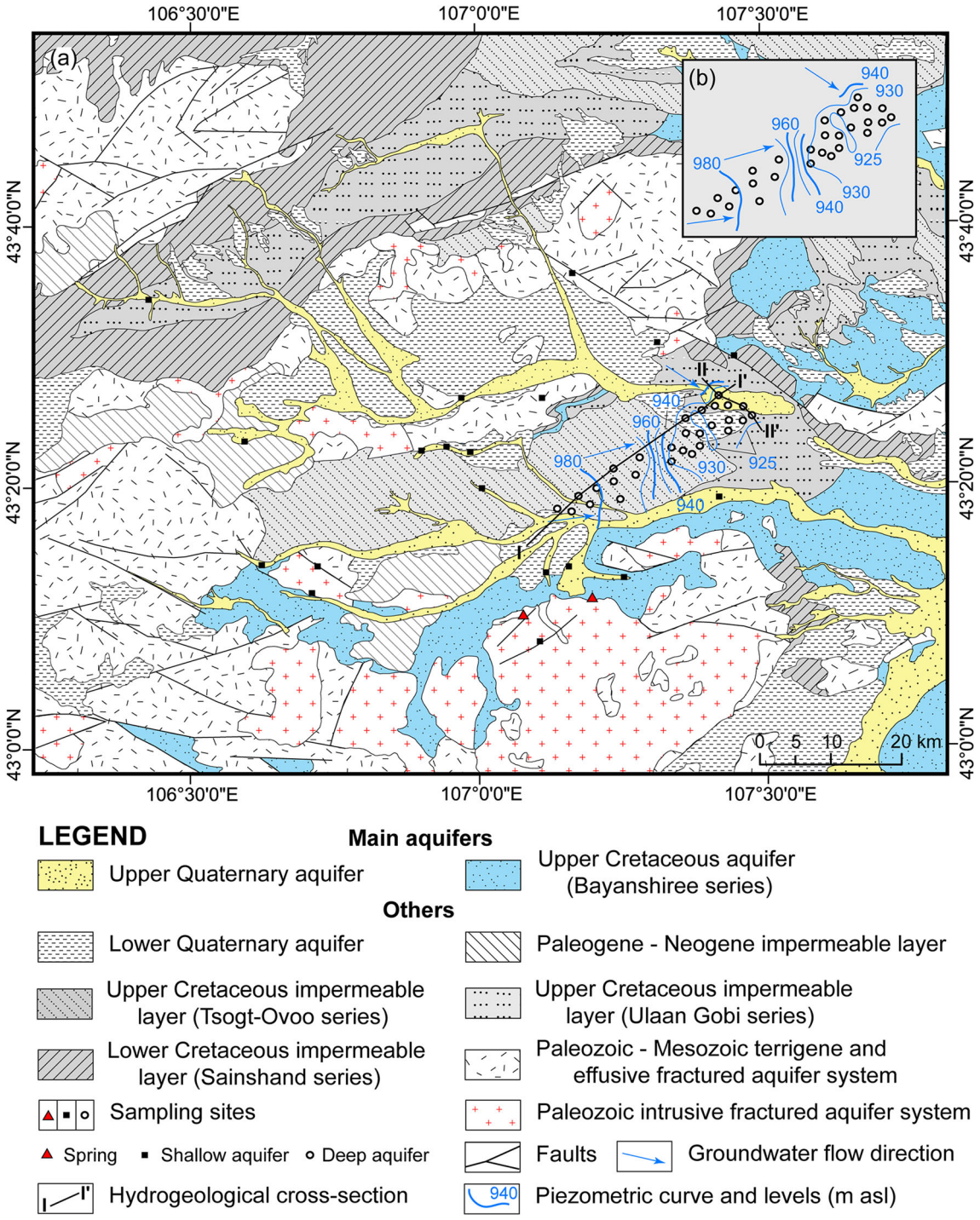

Fig. 3 **a** Hydrogeological map of the study area showing sampling locations (modified after Koldisheva et al. 1986 and Burenkhuu et al. 1995). **b** Piezometric map of Gunii Khooloi aquifer (Tuvdendorj et al. 2008)

(sampled in 100-ml polyethylene bottles, free of bubbles, measured each sampling day, by 0.1-N-sulfuric-acid-titration method with digital titrator (Model 16900, HACH) at an accuracy of ±1%) were also determined in the field.

All sampling equipment was disposable and the sampling procedures for major ions and stable isotopes were performed following the Australian Geoscience method (Sundaram et al. 2009). Samples for laboratory analysis were filtered through 0.45-μm cellulose acetate membrane filters and only those analyzed for cations were stabilized by the addition of 3% HNO_3 in the field. All water samples stored in 50-ml polypropylene, gamma-sterilized centrifuge tubes were free of bubbles and transported at temperatures below 4 °C.

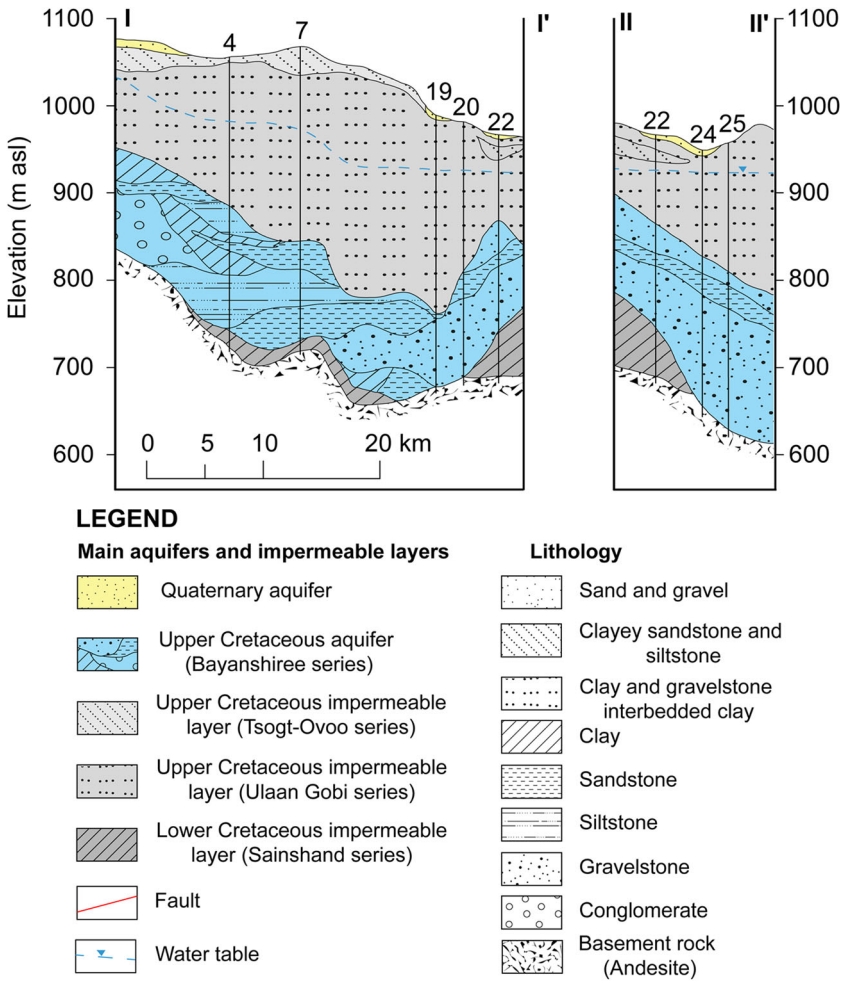

Fig. 4 Hydrogeological cross-section of the Gunii Khooloi basin along transects I–I′ and II–II′ shown in Fig. 3 (modified after Tuvdendorj et al. 2008). The numbers on the surface indicate the sampling sites, as shown in Fig. 1

Major anions (Cl^-, SO_4^{2-}, and NO_3^-) were determined using an ion-chromatography (881 Compact IC pro, Metrohm) with 1% accuracy, and major cation concentrations (Ca^{2+}, Mg^{2+}, Na^+, and K^+) were analyzed using an inductively coupled plasma-atomic emission spectrometer (ICP–AES; Thermo Scientific iCAP 6000 series) with 3% accuracy at the Graduate School of Environmental Studies, Tohoku University, Japan. The analytical error for the measurement of major ions was determined by calculating the ionic charge balance, which was within ±5% for all samples.

All water samples taken for stable isotopes ($\delta^{18}O$ and δD) determination were analyzed using a liquid water isotope analyzer (Picarro, L2120-i) at the Groundwater Research Group in the Geological Survey of Japan (GSJ), National Institute of Advanced Industrial Science and Technology (AIST). The measured results are reported relative to the Vienna Standard Mean Ocean Water (VSMOW) in per mille (δ‰). The analytical precisions for $\delta^{18}O$ and δD are within ±0.1 and ±1‰, respectively.

Fifteen tritium (^3H) samples and 10 radiocarbon isotope samples were collected from the end of June 2017. Water samples for ^3H analysis were collected in 1-L polyethylene bottles. The ^3H compositions were measured using a liquid scintillation counter (Hitachi ALOCA, LSC-LB7) after electrolytic enrichment and samples were analyzed at GSJ. The results were expressed as tritium units (TU) and the analytical error and detection limit were 0.23 and 0.3 TU, respectively.

Samples for radiocarbon analysis were collected in 1 L PAN (BAREX) techno bottles and measured at Beta Analytic Inc, in Miami, Florida, USA. Analysis to determine the $\delta^{13}C$ and ^{14}C values of total inorganic carbon (TIC, ΣCO_2) were measured using isotope ratio mass spectrometry (IRMS) and accelerator mass spectrometry (AMS) by the gas-strip method, respectively. The results for $\delta^{13}C$ are expressed in the conventional δ-per mille (δ‰) notation referenced to the Vienna Pee Dee Belemnite (VPDB) international standard (Craig 1957) and results for ^{14}C are reported as percent modern carbon (pMC). The analytical error was ±0.3‰ for $\delta^{13}C$ and ±0.1 pMC for ^{14}C.

Results

The results of hydrochemical, stable isotopic and tritium analyses of groundwater from the Gunii Khooloi basin are presented in Table 1, and sampling sites are shown in Figs. 1 and 3. Groundwater samples were separated into

Table 1 Field data, major ion concentrations, and stable isotopic compositions of precipitation and groundwater samples in the study area. Locations are shown later in the figures

Sample No.	Sample category	Elevation (m asl)	Well depth (m)	pH	Temp (°C)	EC (μS/cm)	DO (mg/L)	Ca	Mg	Na	K	HCO_3	Cl	SO_4	NO_3	$\delta^{18}O$ ‰ VSMOW	$\delta^{2}H$	d excess	^{3}H (TU)
0	Rain	1,113	-	-	-	-	-	-	-	-	-	-	-	-	-	1.9	4	-11.2	-
1	Deep	1,039	329	7.7	15.5	3,330	5.7	104	16	397	2.0	106	455	433	8	– 10.9	– 95	– 8.1	<0.3
2	Deep	1,046	299	7.9	16.1	3,750	4.2	163	22	621	2.4	84	721	697	10	– 11.0	– 95	– 6.8	-
3	Deep	1,062	245	8.2	16.2	5,750	3.8	255	24	1,027	4.0	38	1,244	1,189	4	– 10.9	– 92	– 4.8	<0.3
4	Deep	1,056	310	8.0	15.3	4,110	5.1	157	32	685	2.6	80	768	811	12	– 11.0	– 95	– 6.6	-
5	Deep	1,051	388	7.9	17.3	3,640	4.1	142	24	606	2.1	87	688	672	11	– 11.1	– 96	– 6.8	-
6	Deep	1,038	379	7.8	17.7	3,580	4.0	141	24	590	2.0	92	673	653	10	– 11.2	– 96	– 6.1	-
7	Deep	1,070	372	7.9	17.4	3,880	4.9	140	33	679	2.1	48	748	726	16	– 10.7	– 95	– 8.9	-
8	Deep	1,037	254	7.8	15.8	2,680	5.7	124	27	425	1.3	102	496	468	14	– 11.2	– 97	– 7.9	-
9	Deep	1,056	367	7.8	18.5	3,720	4.2	161	25	636	2.0	88	740	688	9	– 11.3	– 96	– 5.3	-
10	Deep	1,069	407	8.0	19.7	3,310	3.9	117	24	608	1.8	101	699	638	11	– 11.6	– 96	– 4.0	<0.3
11	Deep	1,028	390	7.9	18.9	3,400	5.9	111	23	595	1.6	103	660	608	11	– 11.6	– 96	– 3.1	<0.3
12	Deep	1,016	394	7.9	19.6	4,740	2.2	204	29	817	1.9	88	951	952	13	– 10.8	– 92	– 6.1	<0.3
13	Deep	1,019	372	7.9	18.5	3,910	3.4	124	27	702	1.6	110	747	749	14	– 11.2	– 94	– 4.3	-
14	Deep	1,008	371	7.9	17.9	3,790	3.7	120	25	667	1.5	104	717	707	14	– 11.3	– 94	– 4.1	-
15	Deep	994	354	7.8	18.6	3,860	5.3	105	31	681	1.4	130	728	702	18	– 11.0	– 93	– 5.7	-
16	Deep	994	365	7.6	17.2	4,970	2.4	280	17	813	1.2	87	1,030	981	8	– 10.4	– 92	– 8.0	-
17	Deep	998	374	7.7	17.3	4,810	3.2	232	23	827	1.4	103	1,114	801	10	– 10.0	– 92	– 11.3	-
18	Deep	978	348	7.8	16.8	5,070	3.0	238	28	856	1.5	115	1,166	823	11	– 10.0	– 91	– 11.5	-
19	Deep	988	291	7.8	16.4	5,140	3.8	261	33	798	1.4	82	1,322	674	12	– 10.3	– 92	– 9.7	<0.3
20	Deep	982	286	7.6	15.5	5,130	5.7	191	43	891	1.4	195	1,170	793	17	– 10.1	– 90	– 9.3	-
21	Deep	964	273	7.7	14.1	4,740	4.4	135	37	989	2.1	247	1,079	849	14	– 10.1	– 88	– 7.1	-
22	Deep	965	269	7.8	13.7	4,840	5.0	112	30	916	2.2	224	987	794	16	– 9.8	– 87	– 8.1	<0.3
23	Deep	956	376	7.8	15.9	6,500	2.3	426	31	1,081	2.9	58	1,665	1,188	4	– 10.6	– 91	– 5.8	-
24	Deep	951	315	8.0	15.3	5,610	3.9	241	39	1,016	2.6	159	1,289	939	14	– 9.7	– 89	– 10.9	<0.3
25	Deep	959	329	7.9	16.6	6,410	4.5	303	58	1,119	2.8	118	1,602	1,016	16	– 9.0	– 87	– 15.5	<0.3
26	Deep	973	358	8.0	16.9	5,550	4.3	246	45	987	2.4	127	1,341	829	17	– 9.7	– 90	– 12.3	-
27	Deep	973	367	8.0	15.9	4,720	5.0	186	36	856	2.0	148	1,068	725	15	– 9.8	– 91	– 12.4	-
28	Deep	968	310	8.1	15.6	4,070	4.0	136	34	729	1.8	152	837	652	16	– 10.3	– 93	– 10.1	-
29	Shallow	1,204	3.2	7.6	16.2	550	4.2	40	7	56	1.1	148	29	35	76	– 11.5	– 82	10.0	-
30	Shallow	1,065	6.4	7.9	10.2	620	5.3	36	10	93	1.1	253	47	38	6	– 10.8	– 78	8.6	-
31	Shallow	1,081	2.1	7.4	14.9	760	2.4	62	11	78	1.0	278	43	54	19	– 10.2	– 76	5.5	-
32	Shallow	1,096	2.6	7.3	14.7	740	1.1	61	12	114	1.4	368	60	56	19	– 10.6	– 78	6.7	-
33	Shallow	1,121	8.2	7.6	16.8	750	4.2	41	6	114	0.4	272	43	59	38	– 10.6	– 75	9.2	25.0
34	Shallow	1,122	3.9	7.7	15.9	900	1.1	28	4	173	1.4	376	34	39	64	– 10.0	– 77	2.2	-
35	Shallow	1,146	8.8	8.0	15.8	990	4.9	22	4	208	0.5	372	41	84	57	– 9.5	– 75	1.2	-

Table 1 (continued)

Sample No.	Sample category	Elevation (m asl)	Well depth (m)	pH	Temp (°C)	EC (µS/cm)	DO (mg/L)	Ca	Mg	Na	K	HCO_3	Cl	SO_4	NO_3	$\delta^{18}O$ ‰ VSMOW	δ^2H	d excess	^3H (TU)
36	Shallow	1,173	4.7	8.1	13.9	830	5.4	26	4	153	0.4	314	34	74	38	− 10.3	− 78	4.2	28.2
37	Shallow	1,237	3.1	7.3	15.4	4,040	2.3	148	4	659	2.7	203	812	647	15	− 10.6	− 89	− 4.6	-
38	Shallow	1,246	4.2	7.8	13.8	1,050	4.1	43	21	129	0.5	264	96	74	91	− 10.1	− 76	5.1	-
39	Shallow	1,282	2.8	8.0	14.3	750	7.9	36	12	89	0.2	169	59	105	30	− 10.2	− 78	3.4	-
40	Shallow	1,290	3.6	7.9	15.4	1,830	4.8	59	17	269	0.9	238	167	273	92	− 11.3	− 87	4.0	-
41	Shallow	1,389	5.3	8.3	14.7	590	6.2	18	4	114	0.4	221	32	52	25	− 9.9	− 73	5.9	-
42	Shallow	1,127	2.3	7.6	15.7	1,430	2.1	39	7	268	0.9	321	134	191	43	− 11.4	− 89	2.0	7.1
43	Shallow	1,105	3.2	7.8	12.7	3,150	3.3	76	20	556	1.4	338	525	367	128	− 10.2	− 80	1.4	19.6
44	Shallow	1,081	5.8	7.7	12.1	1,380	2.9	88	19	172	0.8	153	155	179	125	− 8.1	− 78	− 13.3	-
45	Shallow	1,017	3.8	7.5	13.7	2,000	4.9	80	14	324	0.8	207	299	291	55	− 10.7	− 91	− 5.2	-
46	Shallow	981	4.2	7.9	14.7	1,010	2.8	15	5	201	0.8	323	68	93	28	− 10.5	− 85	− 1.4	-
47	Shallow	977	3.3	7.9	13.2	1,380	3.9	38	8	217	0.3	192	173	158	64	− 11.2	− 85	4.6	3.1
48	Spring	1,188	0.3	8.1	17.6	390	6.9	45	7	26	0.3	171	13	23	10	− 10.2	− 75	6.8	15.7
49	Spring	1,124	-	8.0	10.1	570	5.0	49	7	60	0.2	206	40	50	13	− 10.8	− 82	4.2	-

three representative groups according to the hydrogeological conditions of the Gunii Khooloi basin: springs, shallow groundwater (<10 m bgs, Quaternary streambed aquifer), and deep aquifer or Gunii Khooloi aquifer (>100 m bgs, Cretaceous confined aquifer).

During the investigations conducted in September–October 2016, the groundwater temperature ranged from 10.1 °C (sample 49) to 19.7 °C (sample 10). The mean temperature of the deep groundwater (16.8 °C) was higher than that of shallow groundwater (14.4 °C) and spring water (13.8 °C). The groundwater pH ranged from 7.3 to 8.3 with an average value of 7.8 that indicates a neutral to a slightly alkaline character. The mean pH of the spring water (8.0) was higher than that of the shallow (7.7) and deep groundwater (7.9). Electrical conductivity (EC) increases along the flow directions, with an average of 480 µS/cm in springs and 970 µS/cm in shallow groundwater, with the exception of three samples with EC 4,040 µS/cm (sample 37), 3,150 µS/cm (sample 43), and 2,000 µS/cm (sample 45). Deep groundwater samples exhibit high variability of EC, which ranges from 2,680 µS/cm (sample 8) to 6,500 µS/cm (sample 23) and an average value of 4,465 µS/cm. All groundwater samples contain dissolved oxygen (DO >2 mg/L).

At first inspection, the classification of water quality was conducted using a Piper trilinear diagram (Piper 1944), which is a graphical interpretation of the chemistry of water samples and is extensively used to evaluate the geochemical evolution of groundwater (O'Shea and Jankowski 2006). The shallow groundwater plots were dispersed in the Piper diagram (Fig. 5). In the case of the Gunii Khooloi deep aquifer, water samples were predominantly chloride type, whereas samples from the western part of the aquifer were more sulfate-enriched than the eastern part of the aquifer. The concentrations of major cations in the Gunii Khooloi basin were in the order of Na + K > Ca > Mg. Overall, the trilinear diagram shows that almost all water samples fall into zone 2, which indicates that groundwater in the Gunii Khooloi basin is dominated by alkalis, which exceed alkaline earths.

To examine the relationship between sampling sites and water quality, Stiff diagrams (Stiff 1951) were prepared and are shown on the map in Fig. 6. Spring water samples show $Ca(HCO_3)_2$ or $Na(HCO_3)$ type, while shallow groundwater is mainly characterized by $Na(HCO_3)$ and NaCl type; however, these diagrams are small, which indicates low EC. Although the springs and shallow groundwater are dispersed in the Piper diagram, it is clear that the dispersion reflects a slight change of ion concentrations due to the local conditions of the sampling sites. Only the shallow groundwater samples (Nos. 37, 43, and 45) are NaCl type with high EC; these are located at an outcrop of Cretaceous and Paleozoic-Mesozoic units. In contrast, all deep groundwater samples are classified as NaCl type, with different total dissolved solids (TDS) concentrations between the western and eastern parts. TDS in deep groundwater ranges from 1,660 to 4,460 mg/L. The average TDS concentrations in

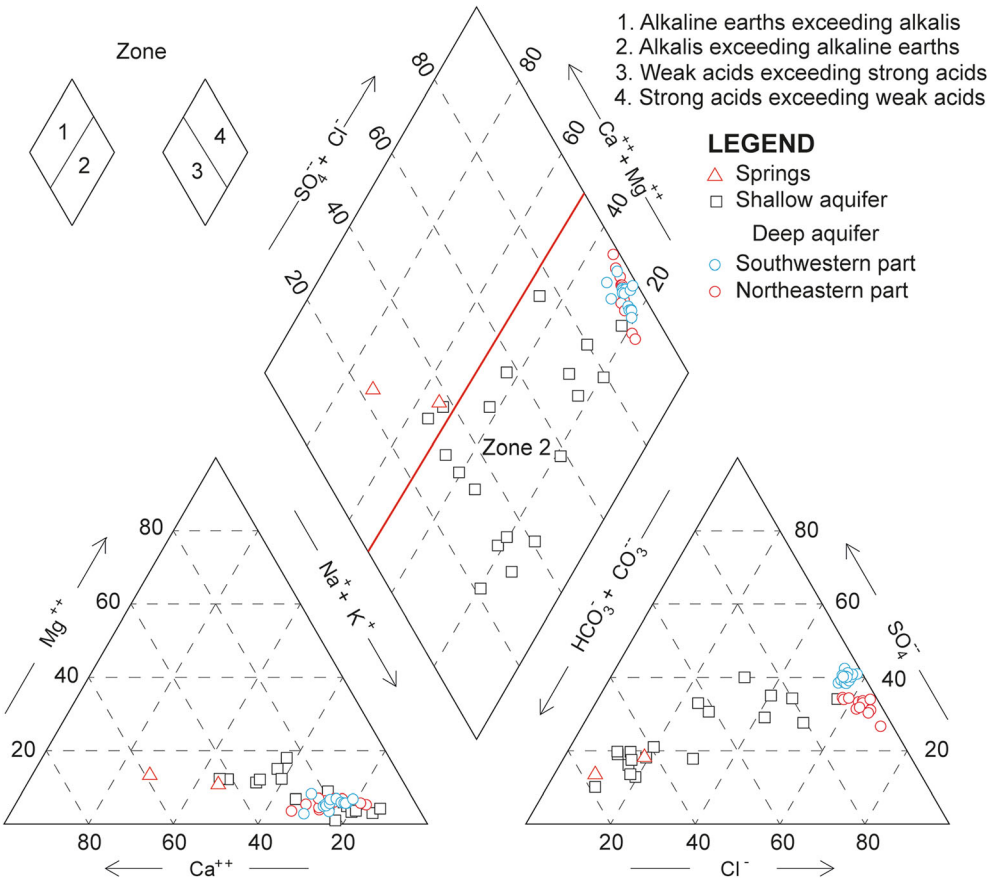

Fig. 5 Piper diagram for the chemical analysis of groundwater collected from the Quaternary and Cretaceous aquifer in the Gunii Khooloi basin

the southern and northern parts of the deep aquifer are 2,440 and 3,400 mg/L, respectively. Combined with the difference in the TDS, a detailed discussion is necessary to consider the groundwater flow from the western to eastern parts.

The Na and Cl concentrations in groundwater show a strong linear relationship (Fig. 7). Such a relationship would be derived from the components of the paleo-ocean (fossil lake) that existed in the Gunii Khooloi basin in geologic age (section 'Geology and hydrogeology'); however, the majority of samples fall above the seawater dilution line, indicating that Na has other sources. Discussion is necessary to consider for groundwater geochemical evolution.

The stable isotope ratio (δD and $\delta^{18}O$) can be a tracer of groundwater origin. Figure 8 shows the relationship between $\delta^{18}O$ and δD for groundwater and precipitation in the study area. The values for all groundwater samples show a range from –11.6 to –8.1‰ for $\delta^{18}O$ and from –97 to –73‰ for δD. The shallow groundwater samples are distributed somewhat sparsely, but seem to concentrate around –77‰ for δD and –10.5‰ for $\delta^{18}O$. The δD content of the deep groundwater tends to be lighter than that of the shallow groundwater (except sample Nos. 37, 44 and 45). The Gunii Khooloi aquifer can be divided into two different groups, depending on the location of sampling sites; the northeastern part of the aquifer (mean values of –95‰ δD and –11.1‰ $\delta^{18}O$) is more enriched than the southwestern part in respect to δD (mean values of –90‰ δD and –10‰ $\delta^{18}O$). The $\delta^{18}O$ and δD values of the precipitation sample were 1.9 and 4‰, respectively.

Tritium (^{3}H) is a radioactive isotope with a half-life of 12.43 years and has been used to distinguish groundwater recharged during the pre-bomb time from younger water (Fontes 1983; Clark and Fritz 1997). ^{3}H activities (Table 1) for spring water and shallow groundwater samples range from 3.1 (sample 45) up to 28.2 TU (sample 36). No significant tritium content could be detected in the deep groundwater samples (<0.3 TU). By simple calculation, approximately 50 years are necessary for ^{3}H to decrease below the quantitative limit from an initial 28.2 TU by radioactive decay.

In the deep groundwater samples, ^{14}C activities (Table 2) were between 0.74 and 3.3 pMC, except for sample Nos. 22 (30.1 pMC) and 24 (14.9 pMC). The $\delta^{13}C$ values mostly range from –6.4 to –8.8‰, except for sample No. 3 (–12.0‰).

Discussion

Groundwater origin

The local meteoric water line (LMWL) in the Gunii Khooloi area has not been established due to a lack of stable isotope

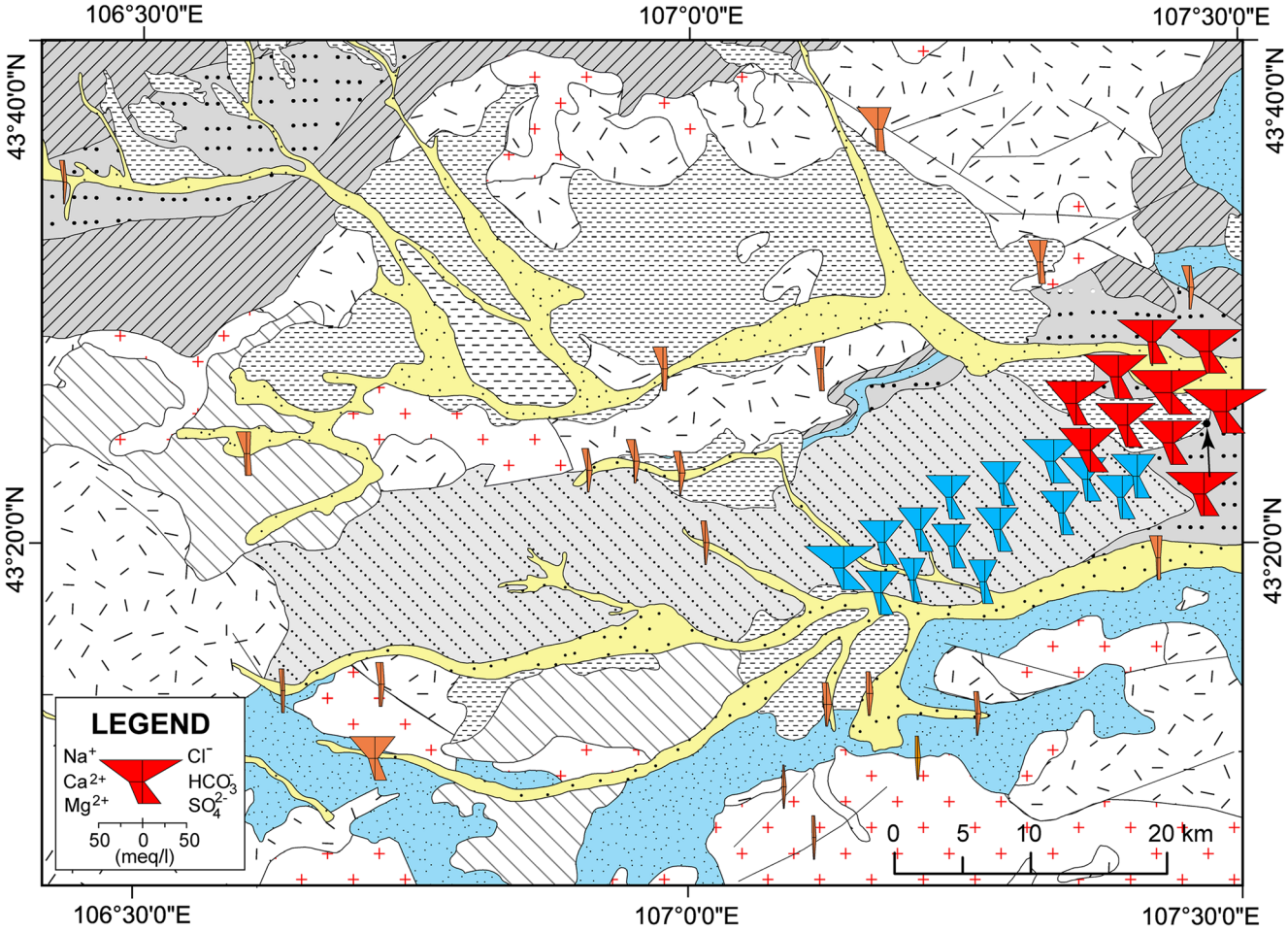

Fig. 6 Shallow and deep groundwater quality represented by Stiff diagrams shown on the hydrogeological map of the study area (refer to Fig. 3 for the hydrogeological map legend). Orange Stiff diagrams indicate the shallow groundwater chemistry, while blue and red Stiff diagrams indicate the deep aquifer chemistry in the southwestern and northeastern part of the Gunii Khooloi aquifer, respectively

data for precipitation. According to data from several meteorological stations around the study area since 1986, including Ulaanbaatar station, Baotou station, Yinchuan station and Zhangye station, taken from the International Atomic Energy Agency (IAEA) database (IAEA/WHO 2018), the δD and $\delta^{18}O$ values in precipitation are highly variable, from −237‰ (Ulaanbaatar) to 5‰ (Yinchuan), and from −30.5‰ (Ulaanbaatar) to 3.9‰ (Yinchuan), respectively. Therefore, it is assumed that the LMWL for the Southern Gobi Region in Mongolia is $\delta D = 7.29\delta^{18}O + 0.48$ (Fig. 8), which is close to the global meteoric water line (GMWL) as determined by Craig (1961). From the weighted mean values obtained from

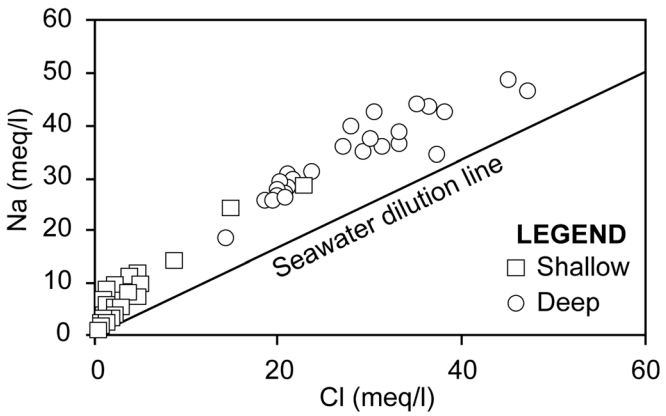

Fig. 7 Relationship between Na and Cl in groundwater samples in the study area

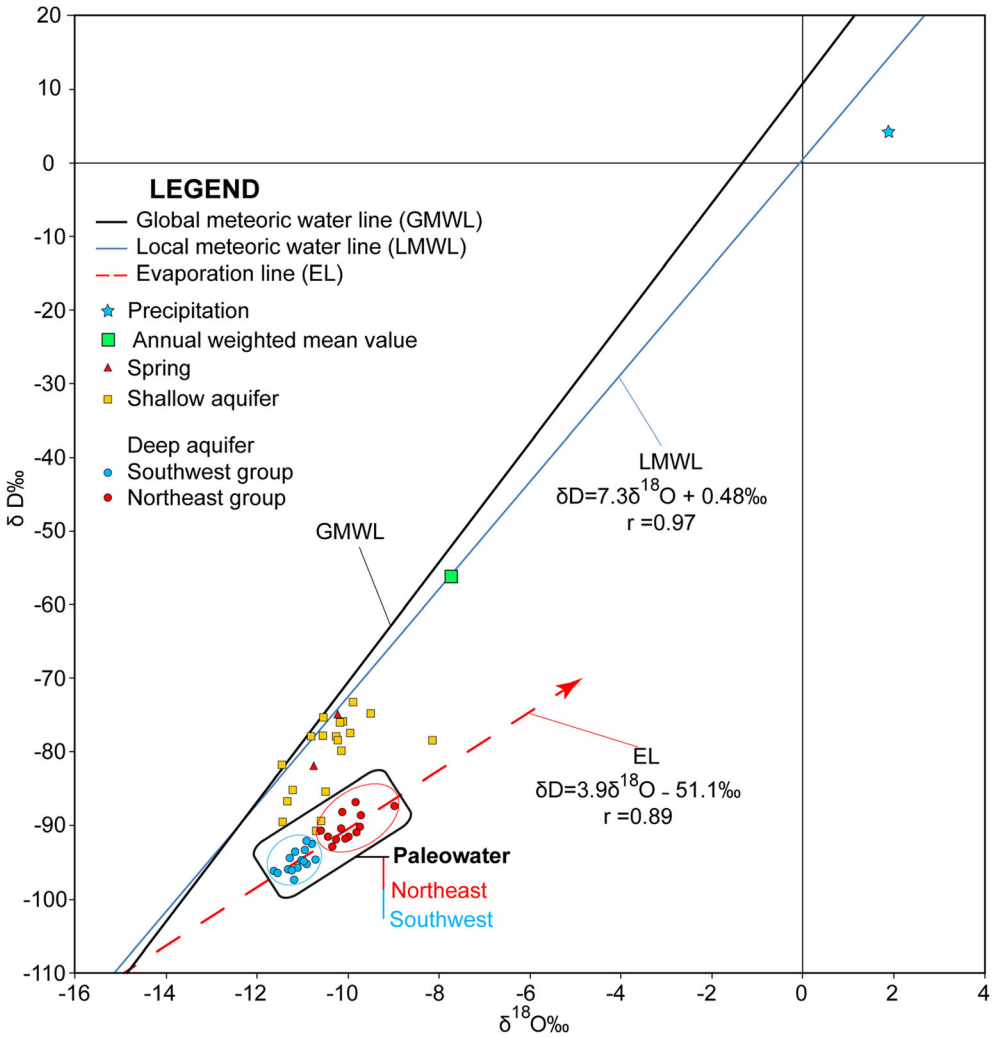

Fig. 8 Plot of $\delta^{18}O$ and δD content for groundwater from the Gunii Khooloi basin, with plots of the GMWL, LMWL and EL

these stations (–7.8‰ for $\delta^{18}O$ and –56‰ for δD) and the precipitation data from the present study, this LMWL seems to be reasonable.

The springs and shallow groundwater samples (except sample Nos. 37, 40, 42, 44–47) fall below the LMWL, which is because the evaporation processes modify the original

Table 2 Radiocarbon results and corrected ^{14}C age for the Gunii Khooloi aquifer

Sample No.	$\delta^{13}C$ (‰ VPDB)	^{14}C (pMC)	Uncorrected age (years)	Tamers model age (years)	Ingerson and Pearson model age (years)	Average age (years)
1	– 7.6	2.25	30,500	26,000	22,000	24,000
2	– 7.4	2.56	29,450	25,000	20,000	22,500
3	– 12.0	3.28	27,450	23,000	22,000	22,500
6	– 7.8	0.96	37,320	33,000	29,000	31,000
10	– 8.8	0.74	39,430	35,000	32,000	33,500
12	– 8.1	1.57	33,380	29,000	25,000	27,000
19	– 8.0	1.49	33,780	29,000	25,000	27,000
22	– 8.7	30.14	9,630	4,400	1,200	2,800
24	– 8.2	14.91	15,290	10,000	7,000	8,500
25	– 6.4	0.81	38,720	34,000	29,000	31,500

δD-$\delta^{18}O$ relationship of the rainfall that results in slopes lower than 8, as reported in many arid regions (Gat 1980; Clark and Fritz 1997; Benjamin et al. 2004; Pang et al. 2011). The deuterium excess (Dansgaard 1964) shows a significant difference between the shallow and deep aquifers, ranging from –15.5 to +10.0‰. Some shallow groundwater samples have low deuterium excess values, which may be influenced by evaporation before or during infiltration. The degree of this influence could be the reason for the relatively high EC of the spring water.

It is noted that deep groundwater in the Gunii Khooloi basin has significantly lighter δD composition than the shallow groundwater (except for sample Nos. 37, 40, 42 and 44–47). The depleted isotopic signatures are considered to be originated from paleowater (during the late Pleistocene; definition after Edmunds 2001), when the climate was colder and wetter than the present day. Such phenomena have been reported in previous studies on the Gobi Desert, Northern China, the Badain Jaran Desert (Gates et al. 2008), Dunhuang basin (Ma et al. 2013), the Ejina basin (Su et al. 2009), Heihe River basin (Zhu et al. 2008), Minqin basin (Edmunds et al. 2006) and Shiyang River basin (Ma et al. 2010). The clusters of deep groundwater seem to form a line with a regression equation of $\delta D = 3.9\delta^{18}O - 51.1‰$ (correlation coefficient: $r = 0.89$). Although the slope of 3.9 is indicative of an evaporation line, the relationship of the two clusters is still not clear. These isotopic compositions are typical for waters that have been affected by evaporation before recharging in a closed basin (Kamel et al. 2008) and in paleo lakes where the isotope composition remains in the pore water of the aquitard (Ortega-Guerrero et al. 1997).

Groundwater age

The main recharge of shallow groundwater in the Gunii Khooloi basin is via precipitation, which is also the main input source of ^3H in groundwater. The global network of stations that monitor isotopes in precipitation does not include the Gunii Khooloi area and IAEA monitoring stations are far from the study area; however, ^3H concentrations are available from 1986 to 2003 at Ulaanbaatar station (in Mongolia), Baotou station (in China), Yinchuan station (in China) and Zhangye station (in China). Detailed data are not available for these regions before 1986; thus, it is imperative to reconstruct missing data to infer what the historic distribution of ^3H has been in precipitation in the study area. The earlier tritium data for the Baotou, Yinchuan and Zhangye stations were reconstructed for northern China (Li et al. 2008; Ma et al. 2008; Liu et al. 2014). These reconstructed ^3H data are very informative and can be used to assist in the interpretation of the relative age dating in the study area.

According to the reconstructed data, the ^3H values for shallow groundwater (15-30 TU) in the study area clearly characterizes these waters as natural background, derived from very new surface runoff in the stream network. For sample Nos. 47 and 42, lower ^3H concentrations of 3.1 and 7.1 TU were measured. They can be classified as modern groundwater, as defined by Edmunds (2001), but seem somewhat older. By simple calculation, their ages are estimated as more than 25 years.

Groundwater in the Cretaceous deep aquifer with relatively low tritium content was supposed to be recharged before 1952, and therefore the ^{14}C method was applied to these waters. To obtain adjusted ^{14}C ages, it is necessary to know the initial ^{14}C activity of recharge water. However, estimation of the initial ^{14}C activity is a complicated task and several correction models have been applied to calculate it (Ingerson and Pearson 1964; Tamers 1967; Vogel 1970; Mook 1976; Fontes and Garnier 1979).

In the current study, soil CO_2, organic matter and carbonate minerals are considered as the carbon sources in the groundwater. The Gunii Khooloi aquifer does not seem likely to contain much organic matter because of high dissolved oxygen, as shown in Table 1 (Winograd and Robertson 1982); therefore, the soil CO_2 and carbonate minerals are assumed to be the primary sources of carbon in the groundwater. Detailed information about ^{14}C in the unsaturated zone and in saturated part of the aquifer is not available; thus, it is for these reasons that the Tamers (1967) model and Ingerson and Pearson (1964) model were used to determine the ^{14}C age. In both models, the ^{14}C content in the initial water (in this case, recharging water in the past) is assumed to be formed by mixing of soil CO_2 and carbon dissolved from carbonate minerals. The ^{14}C content in the initial water is obtained from the concentrations of carbon species in the Tamers model, while the same is obtained from $\delta^{13}C$ in the Ingerson and Pearson model. Calculations were performed using NETPATH (Plummer et al. 1994).

Both ages are very similar, which supports the preceding assumption. The average age of groundwater in the Cretaceous aquifer increases from approximately 22,500 years old (sample Nos. 2 and 3) to more than 33,500 years old (sample No. 10) along the groundwater flow direction up to the central part of the deep aquifer (Table 2). Samples collected from the central part of the Cretaceous aquifer are 27,000 years of age (sample Nos. 12 and 19). The age of the central part of the aquifer is highly influenced by younger groundwater flow which is distributed in the northeastern part of the aquifer. The average age of the groundwater in the northeastern part of the Cretaceous aquifer is much younger (except sample No. 25) than the southwestern part of the aquifer and increases from northwest to southwest. These results support that deep groundwater was recharged during the last glacial age. The deep groundwater shows a very old age, although the EC increases along the groundwater flow path.

The same tendency has been observed in semi-arid and arid basins around the world such as the northern Sahara sedimentary basin in Algeria (Guendouz et al. 2003), the Chahardouly alluvial basin in West Iran (Tizro and Voudouris 2008), as well

as other groundwater basins in the Gobi Desert (northern China part) such as the Minqin Basin (Zhu et al. 2007), the Heihe River Basin (Yang et al. 2011), the Dunhuang Basin (Ma et al. 2013) and the Ejina Basin (Wang et al. 2013).

The ^{14}C ages from sample Nos. 2 and 10 can be used to estimate the maximum groundwater flow velocity. The older sample (33,500 years) is approximately 12.2 km further along the flow path from the younger sample (22,500 years), which indicates an approximate flow velocity of 1.11 m/year. Assuming an average porosity of 0.3 (Tuvdendorj et al. 2008), the groundwater flux can be calculated as 0.33 m/year. On the other hand, using Darcy's Law, the estimated groundwater velocity between sample Nos. 2 and 10, assuming hydraulic conductivity of 3.7 m/day and a hydraulic gradient of 3.3×10^{-4} (Tuvdendorj et al. 2008), is 1.48 m/year. The result is basically concordant with that calculated by ^{14}C dating, and indicates that the Cretaceous deep confined aquifer flow is relatively slow and the water resources are essentially non-renewable in the Gunii Khooloi aquifer.

Conceptual model

Based on this first analysis of the isotopic and hydrogeochemical data, a conceptual model of groundwater recharge, flow and geochemical evolution is proposed to further understand the hydrogeological conditions in the Gunii Khooloi basin (Fig. 9). Quaternary unconsolidated sand, cobbles and gravel sediments form the shallow streambed aquifer, which is recharged by local precipitation in the Gunii Khooloi basin; however, in arid regions with low precipitation and high evaporation, the diffuse recharge is limited. In the Elgen and Gurvan Kharaat Mountain area, the isotopic compositions of the shallow groundwater tend to conform to patterns similar to the deep confined aquifer, which indicates that those areas could be the recharge area of the deep confined Cretaceous aquifer. In contrast, the shallow groundwater stable isotope ratio and tritium data in the Duulga Mountain area are different from the others. It should be noted that the shallow aquifer and deep aquifer are totally different aquifer systems in the Gunii Khooloi basin.

In the deep confined Cretaceous aquifer, the groundwater recharge mechanism is relatively complex. According to climatic conditions, it is difficult to reason that recharge occurs in the deep aquifer today, even though approximately 1.5 m/year of groundwater flow was calculated by ^{14}C and the hydrogeological conditions. Therefore, the groundwater must be stagnant today but flowed during the last glacial age, which is supported by the light δD and $\delta^{18}O$ content in most of the

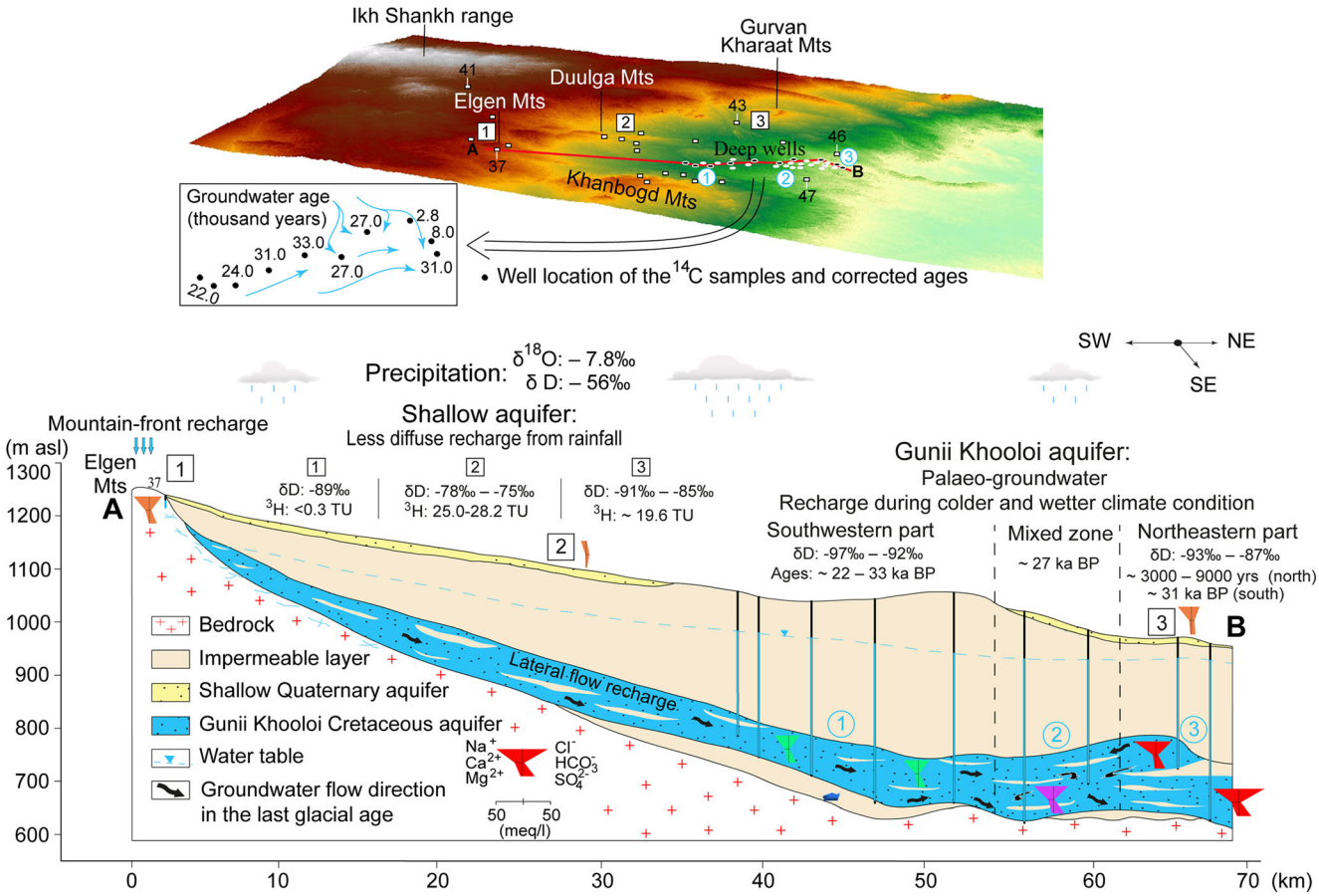

Fig. 9. Conceptual hydrogeological and hydrogeochemical model of the Gunii Khooloi basin.

confined groundwater samples, and by their ^{14}C age. Furthermore, the water quality distribution, ^{14}C and groundwater flow direction indicate that groundwater flows from southwest to northeast in the southwestern part of the aquifer, while groundwater mainly comes from the northwest and flows into the southeastern part of the aquifer. The piezometric map (Fig. 3b) supports these results. Between these areas, groundwater is mixed and goes through the study area in the southeast direction. Therefore, according to geological evolution, the study area was of a Paleo-Asian Ocean margin setting (Fig 2b) and stable isotope results showed deep groundwater is affected by evaporation (paleowater). This is one of the pieces of evidence that deep groundwater originated from a fossil lake, non-renewable and with no genetic relationship to modern recharge.

Conclusions

Geochemical and isotopic tracers were used to understand the groundwater origin and hydrogeochemical characteristics of groundwater in the Gunii Khooloi basin, which is located in the Southern Gobi Region of Mongolia. Spring water in the Gunii Khooloi basin is classified as Ca-Na-HCO_3 or Na-Ca-HCO_3 type and shallow groundwater is characterized by Na-Ca-HCO_3, Na-mixed and Na-Cl-SO_4 water types. In contrast, deep groundwater is characterized by Na-Cl-SO_4 to Na-Cl water types.

Based on the stable isotope compositions, groundwater in the Gunii Khooloi basin has a meteoric water origin. The deep confined aquifer is significantly depleted in heavy isotopes compared with the Quaternary shallow aquifer and modern rainfall. Thus, the stable isotope results clearly imply that there is no direct recharge connection between the deep confined aquifer and direct modern recharge. Deep groundwater is also mainly paleowater that was formed under colder and wetter climate conditions during the late Pleistocene and Holocene period. This phenomenon is confirmed by the ^{14}C age (2.8–33.5 ka) and it is common in arid regions.

The results of this study have significant implications with respect to developing a conceptual model, to water resources management, and to the identification of groundwater origin and age in the Gunii Khooloi basin and other water-stressed basins in the Southern Gobi Region of Mongolia. These results will facilitate the management of water usage and the design groundwater monitoring systems, to confirm assessment of the groundwater resources in this region. Further studies within the Gunii Khooloi basin are currently in progress, including geochemical evolution and groundwater quality.

Acknowledgments The authors thank Oyu Tolgoi Mine's hydrogeologist P. Uuganbayar for help and advice during this study, and we thank his team in the Oyu Tolgoi mine for giving us the opportunity to collect water samples from deep production wells of the Gunii Khooloi aquifer. We thank editor Martin Appold, associate editor Randy Scotler, technical editorial advisor Sue Duncan and two anonymous reviewers for their constructive suggestions, comments and kind corrections.

Funding information The Authors are grateful to the Japan International Cooperation Agency (JICA) for granting the first author a study fellowship ("KIZUNA" project) to carry out his doctorate research work at Tohoku University, Japan.

References

Badarch G, Cunninghamb WD, Windley BF (2002) A new terrane subdivision for Mongolia: implications for the Phanerozoic crustal growth of Central Asia. J Asian Earth Sci 21:87–110

Bahir M, Ait Tahar M, Goumih A, Ouhamdouch S, Rouissa A (2018) Impact of mine polymetallic Draa Sfar South on the aquifer of central Haouz (Morocco). J Mater Environ Sci 9:1405–1410

Benjamin L, Knobel LL, Hall LF, Cecil LD, Green JR (2004) Development of a local meteoric water line for southeastern Idaho, western Wyoming, and south-central Montana. US Geol Surv Sci Invest Rep 2004–5126

Burenkhuu E, Gotovsuren A, Badarch G, Davgatseren A (1995) Complex geological map of Galbiin Govi Area, 1:200 000 (in Mongolian). Open File Report 4877, Geological Fund of Mongolia, Ulaanbaatar, Mongolia

Chen F, Wu D, Chen J, Zhou A, Yu J, Shen J, Wang S, Huang X (2016) Holocene moisture and East Asian summer monsoon evolution in the northeastern Tibetan Plateau recorded by Lake Qinghai and its environs: a review of conflicting proxies. Quat Sci Rev 154:111–129

Clark I, Fritz P (1997) Environmental isotopes in hydrogeology. Lewis, Boca Raton, FL

Coplen TB, Herczeg AL, Barnes C (2000) Isotope engineering-using stable isotopes of the water molecule to solve practical problems. In: Cook PG, Herzeg A (eds) Environmental tracers in subsurface hydrology. Kluwer, Boston, pp 79–110

Craig H (1957) Isotopic standards for carbon and oxygen and correction factors for mass-spectrometric analysis of carbon dioxide. Geochim Cosmochim Acta 12:133–149

Craig H (1961) Isotopic variations in meteoric waters. Science 133:1702–1703

Dansgaard W (1964) Stable isotopes in precipitation. Tellus 16:436–468

Edmunds WM (2001) Palaeowaters in European coastal aquifers: the goals and main conclusions of the PALAEAUX project. In: Edmunds WM, Milne CJ (eds) Paleowaters in coastal Europe: evolution of groundwater since the late Pleistocene. Geol Soc London Spec Publ 189:1–16

Edmunds WM, Ma JZ, Aeschbach-Hertig W, Kifter R, Darbyshire DPF (2006) Groundwater recharge history and hydrogeochemical evolution in the Minqin Basin, North West China. Appl Geochemistry 21:2148–2170

Felauer T, Schlütz F, Murad W, Mischke S, Lehmkuhl F (2012) Late Quaternary climate and landscape evolution in arid Central Asia: a multiproxy study of lake archive Bayan Tohomin Nuur, Gobi Desert, southern Mongolia. J Asian Earth Sci 48:125–135

Fontes J-C, Garnier J-M (1979) Determination of the initial 14C activity of the total dissolved carbon: a review of the existing models and a new approach. Water Resour Res 15:399–413

Fontes J (1983) Dating of groundwater. In: Guidebook on nuclear techniques in hydrology. Technical Report Series no. 91. IAEA, Vienna, pp 285–317

Gat J (1980) The isotopes of hydrogen and oxygen in precipitation. In: Fritz P, Fontes JC (eds) Handbook of environmental isotope geochemistry, vol 1. The terrestrial environment. Elsevier, Amsterdam, pp 21–47

Gates JB, Edmunds WM, Darling WG, Ma JZ, Pang ZH, Young AA (2008) Conceptual model of recharge to southeastern Badain Jaran Desert groundwater and lakes from environmental tracers. Appl Geochem 23:3519–3534

Glynn PD, Plummer LN (2005) Geochemistry and the understanding of ground-water systems. Hydrogeol J 13:263–287

Guendouz A, Moulla AS, Edmunds WM, Zouari K, Shand P, Mamou A (2003) Hydrogeochemical and isotopic evolution of water in the Complexe Terminal aquifer in the Algerian Sahara. Hydrogeol J 11:483–495

IAEA/WHO (2018) Global Network of Isotopes in Precipitation: the GNIP Database. https://nucleus.iaea.org/wiser. Accessed 24 January 2018

Ingerson E, Pearson F (1964) Estimation of age and rate of motion of groundwater by the 14C-method. In: Recent researches in the fields of atmosphere, hydrosphere, and nuclear geochemistry. Sugawara Festival Volume. Maruzen, Tokyo, pp 263–283

Jahn B, Wu F, Chen B (2000) Granitoids of the Central Asian Orogenic Belt and continental growth in the Phanerozoic. Trans R Soc Edinb Earth Sci 91:181–193

Kamel S, Younes H, Chkir N, Zouari K (2008) The hydrogeochemical characterization of ground waters in Tunisian Chott's region. Environ Geol 54:843–854

Koldisheva RY, Efimova DV, Grishina AP (1986) Hydrogeological map of the south eastern Mongolia, K-48-B, 1:500 000 (in Russian). Open File Report 3959, Geological Fund of Mongolia, Ulaanbaatar

Kovalenko VI, Yarmoluyk VV, Sal'nikova EB, Kozlovsky AM, Kotov AB, Kovach VP, Savatenkov VM, Vladykin NV, Ponomarchuk VA (2006) Geology, geochronology, and geodynamics of the Khan Bogd Alkali Granite Pluton in southern Mongolia. Geotectonics 40:450–466

Lehmkuhl F, Grunert J, Hülle D, Batkhishig O, Stauch G (2018) Paleolakes in the Gobi region of southern Mongolia. Quat Sci Rev 179:1–23

Li X, Zhang L, Hou X (2008) Use of hydrogeochemistry and environmental isotopes for evaluation of groundwater in Qingshuihe Basin, northwestern China. Hydrogeol J 16:335–348

Liu J, Chen Z, Wei W, Zhang Y, Li Z, Liu F, Guo H (2014) Using chlorofluorocarbons (CFCs) and tritium (^{3}H) to estimate groundwater age and flow velocity in Hohhot Basin, China. Hydrol Process 28:1372–1382

Ma JZ, Wang XS, Edmunds WM (2005) The characteristics of groundwater resources and their changes under the impacts of human activity in the arid Northwest China: a case study of the Shiyang River Basin. J Arid Environ 61:277–295

Ma JZ, Ding Z, Gates JB, Su Y (2008) Chloride and the environmental isotopes as the indicators of the groundwater recharge in the Gobi Desert, northwest China. Environ Geol 55:1407–1419

Ma JZ, Ding Z, Edmunds WM, Gates JB, Huang T (2009) Limits to recharge of groundwater from Tibetan plateau to the Gobi Desert: implications for water management in the mountain front. J Hydrol 364:128–141

Ma JZ, Pan F, Chen L, Edmunds WM, Ding Z, He J, Zhou K, Huang T (2010) Isotopic and geochemical evidence of recharge sources and water quality in the Quaternary aquifer beneath Jinchang city, NW China. Appl Geochem 25:996–1007

Ma JZ, He JH, Qi S, Zhu GF, Zhao W, Edmunds WM, Zhao YP (2013) Groundwater recharge and evolution in the Dunhuang Basin, northwestern China. Appl Geochem 28:19–31

Mahlknecht J, Schneider JF, Merkel BJ, Navarro de Leon I, Bernasconi SM (2004) Groundwater recharge in a sedimentary basin in semi-arid Mexico. Hydrogeol J 12:511–530

Mook W (1976) The dissolution-exchange model for dating groundwater with ^{14}C. In: Interpretation of environmental isotope and hydrochemical data in groundwater hydrology. International Atomic Energy Agency (IAEA), Vienna, pp 213–225

Munkhbaatar N, Sanjdorj S, Ulziibayar G, Chuluunbaatar S (2004) Groundwater exploration report for Oyu Tolgoi process water supply in the Gunii Khooloi and Galbiin Gobi region (in Mongolian). Open File Report, Ministry of Nature and Environment, Ulaanbaatar, Mongolia, pp 23–31

O'Shea B, Jankowski J (2006) Detecting subtle hydrochemical anomalies with multivariate statistics: an example from "homogeneous" groundwaters in the Great Artesian Basin, Australia. Hydrol Process 20:4317–4333

Ortega-Guerrero A, Cherry JA, Aravena R (1997) Origin of pore water and salinity in the lacustrine aquitard overlying the regional aquifer of Mexico City. J Hydrol 197:47–69

Ouhamdouch S, Bahir M, Souhel A, Paula C (2016) Vulnerability and impact of climate change processes on water resource in semi-arid areas: in Essaouira basin (Morocco). In: Grammelis P (ed) Energy, transportation and global warming, green energy and technology. Springer, Cham, Switzerland, pp 719–736

Ouhamdouch S, Bahir M, Carreira PM (2018) Impact du changement climatique sur la ressource en eau en milieu semi-aride: exemple du bassin d'Essaouira (Maroc) [Impact of climate change on semi-arid water resources: example of the Essaouira Basin (Morocco)]. Rev Sci l'eau 31:13–27

Pang Z, Kong Y, Froehlich K, Huang T, Yuan L, Li Z, Wang F (2011) Processes affecting isotopes in precipitation of an arid region. Tellus, Ser B Chem Phys Meteorol 63:352–359

Piper AM (1944) A graphic procedure in the geochemical inter-relation of water analyses. Trans Am Geophys Union 25:914–928

Plummer LN, Prestemon EC, Parkhurst DL (1994) An interactive code (NETPATH) for modeling NET geochemical reactions along a flow PATH, version 2.0. US Geol Surv Water Resour Invest Rep 94-4169, 130 pp. https://doi.org/10.3133/wri944169

Ragab R, Prudhomme C (2002) Climate change and water resources management in arid and semi-arid regions: prospective and challenges for the 21st century. Biosyst Eng 81:3–34

Şengör AM, Natal'in BA, Burtman VS (1993) Evolution of the Altaid tectonic collage and Paleozoic crustal growth in Eurasia. Nature 364:299–307

Stauch G (2016) Multi-decadal periods of enhanced aeolian activity on the north-eastern Tibet Plateau during the last 2 ka. Quat Sci Rev 149:91–101

Stiff HAJ (1951) The interpretation of chemical water analysis by means of patterns. J Pet Technol 3:15–17

Su YH, Zhu GF, Feng Q, Li ZZ, Zhang FP (2009) Environmental isotopic and hydrochemical study of groundwater in the Ejina Basin, northwest China. Environ Geol 58:601–614

Sundaram B, Feitz AJ, de Caritat P, Plazinska A, Brodie RS, Coram J, Ransley T (2009) Groundweater sampling and analysis: a field guide. Geoscience Australia Record 2009(27):95

Tamers M (1967) Surface-water infiltration and groundwater movement in arid zones of Venezuela. Isotopes in Hydrology, Proceedings Series, International Atomic Energy Agency (IAEA), Vienna, pp 339–351

Tizro TA, Voudouris KS (2008) Groundwater quality in the semi-arid region of the Chahardouly basin, West Iran. Hydrol Process 22: 3066–3078

Tuvdendorj A, Sanjdorj S, Ulziibayar G (2008) Report on groundwater exploration in the Gunii Khooloi Deposit (in Mongolian). Open File Report, Ministry of Nature and Environment, Ulaanbaatar, Mongolia, pp 22–30

Vogel J (1970) Carbon-14 dating of groundwater. In: Proceedings of a symposium on isotope hydrology. International Atomic Energy Agency (IAEA), Vienna, pp 225–239

Wang P, Yu J, Zhang Y, Liu C (2013) Groundwater recharge and hydrogeochemical evolution in the Ejina Basin, northwest China. J Hydrol 476:72–86

Wang L, Dong Y, Xu Z (2017) A synthesis of hydrochemistry with an integrated conceptual model for groundwater in the Hexi Corridor, northwestern China. J Asian Earth Sci 146:20–29

Windley BF, Alexeiev D, Xiao W, Kroner A, Badarch G (2007) Tectonic models for accretion of the Central Asian Orogenic Belt. J Geol Soc London 164:31–47

Winograd IJ, Robertson FN (1982) Deep oxygenated ground water: anomaly or common occurrence? Science 216(80):1227–1230

Yang Q, Xiao H, Zhao L, Yang Y, Li C, Zhao L, Yin L (2011) Hydrological and isotopic characterization of river water, groundwater, and groundwater recharge in the Heihe River basin, northwestern China. Hydrol Process 25:1271–1283

Yang X, Scuderi LA (2010) Hydrological and climatic changes in deserts of China since the late Pleistocene. Quat Res 73:1–9

Zhu GF, Li ZZ, Su YH, Ma JZ, Zhang YY (2007) Hydrogeochemical and isotope evidence of groundwater evolution and recharge in Minqin Basin, Northwest China. J Hydrol 333:239–251

Zhu GF, Su YH, Feng Q (2008) The hydrochemical characteristics and evolution of groundwater and surface water in the Heihe River Basin, northwest China. Hydrogeol J 16:167–182